29 March 1996

ELSEVIER

Chemical Physics Letters 251 (1996) 259–267

CHEMICAL PHYSICS LETTERS

Photophysical properties of cyanine dyes in sol–gel matrices

U. De Rossi [a], S. Daehne [a], R. Reisfeld [b,1]

[a] *Federal Institute for Materials Research and Testing, Laboratory for Time-Resolved Spectroscopy, Rudower Chaussee 5, 12489 Berlin, Germany*

[b] *Department of Inorganic Chemistry, The Hebrew University, 91904 Jerusalem, Israel*

Received 21 August 1995; in final form 29 January 1996

Abstract

Planar and twisted cyanine dyes with different pK_a values are examined concerning their protonation equilibrium in sol–gel matrices. In the sol–gel matrix the equilibrium between the cation and the dicationic form shifts to the dication pointing to acid–base reactions of sol–gel walls with cyanine dyes. The colorless dicationic species is not found for pseudoisocyanine and in sol–gel bulks prepared with drying control chemical agents (DCCA) indicating the absence of the responsible interaction. The fluorescence lifetimes of cyanine molecules are used to compare the pore size and distribution in sol–gel matrices prepared with and without DCCA. J-aggregation, examined for one dye, depends strongly on environment polarity and pore size.

1. Introduction

The sol–gel process has attracted increasing attention lately. High-quality glasses for optical applications can be obtained using this low-temperature technique [1] which prevents thermal damaging of the dyes [2]. The immobilization of molecules in sol–gel matrices has the possibility of affecting the intermolecular interactions and photophysical properties of dyes [3]. Embedding organic dyes in such matrices increases their photostability as compared to solutions or organic polymers. An important parameter when incorporating dyes in sol–gel matrices is the interaction between the silica cages and trapped dyes which is examined by the photochromic [4] and spectral behavior of the dyes [5,6]. A large quantity of dyes incorporated in sol–gel matrices have been examined [7–10] but experience with cyanine dyes is scarce although the immobilization of long chain polymethine dyes may be important to their use as a laser medium for the near infrared wavelength region [11]. Recently, attempts to incorporate a dicarbocyanine dye into a sol–gel matrix failed due to the formation of a colorless species [12] probably caused by an attack of silanol groups in the pores.

Cyanine dyes exhibit another important feature: their ability to form J-aggregates. J-aggregates are ensembles of coupled dye molecules with specific photophysical properties such as short radiative lifetime [13] and an intense narrow absorption and emission band red-shifted with respect to the monomer transition [14]. They are widely used as spectral sensitizers for photographic emulsions and are of interest for electro-optical devices due to their

[1] Enrique Berman Professor of Solar Energy.

PII S0009-2614(96)00117-0

high third-order optical susceptibility [15]. For these applications physical immobilization of J-aggregates is superior to LB layers [16] and polymer matrices [17] because of the high mechanical and photophysical stability of the glasses. Using the sol–gel matrix control of the amount of aggregation is possible since the sol–gel process allows a changing of the pore size and polarity of the environment.

We chose different cyanine dyes in order to get information on the protonation equilibria of cyanine dyes in sol–gel matrices. By comparing the properties with those in solution, information about the matrix acidity can be likewise obtained. Different preparation methods were tested to incorporate cyanine dyes and for one dye, to control J-aggregation in the sol–gel matrix. Also, the influence of *drying control chemical agents* (DCCAs) such as formamide and dimethylsulfoxide commonly used to prevent crack formation in glass [18], on protonation and pore size were examined. Differences in pore size can be detected by the emission lifetimes of cyanine dyes since they are sensitive to geometrical restrictions [19].

2. Experimental

For the sol–gel preparation, the following reagents were used: (1) tetramethoxysilane (TMOS; from Fluka), (2) dimethylsulfoxide, (3) formamide, (4) ethanol, (5) KOH, (6) HCl, (7) NH_4OH, (8) HNO_3 (all from Aldrich), (9) doubly distilled water. Different concentration ratios of TMOS, ethanol and water as well as different catalysts were used for the glass preparation. The typical sol–gel preparation was as follows (deviations from this procedure are mentioned in the text): 2 mL TMOS, 2.8 mL ethanol, 1 mL water, 1 mL KOH (0.1N), 2 mL ethanolic dye solution
(dye concentrations: 10^{-3}–10^{-4} mol/L).

When DCCAs were used we added another 2 mL of formamide or dimethylsulfoxide. The solutions were allowed to dry in the dark at room temperature for several months (some samples were stored simultaneously at 60°C for 3 months) since high temperatures may damage the cyanine dyes. The influence of polar media on the aggregation behavior and on dye protonation was tested exposing samples to ammonia atmosphere during gelation. We restricted ourselves to the preparation of bulk glasses rather than thin films allowing the detection of small amounts of the dye because of the larger thickness as compared with glassy films.

The formulae of the cyanine dyes used are shown below.

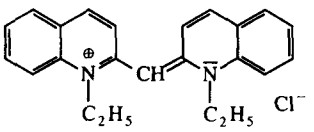

Dye 1 (PIC)

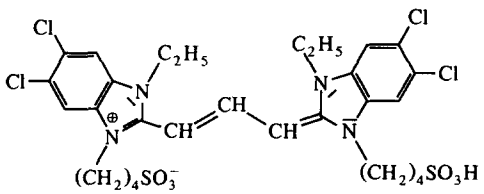

Dye 2 (TDBC)

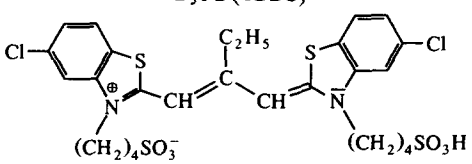

Dye 3

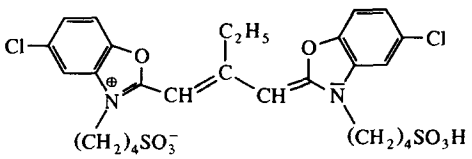

Dye 4

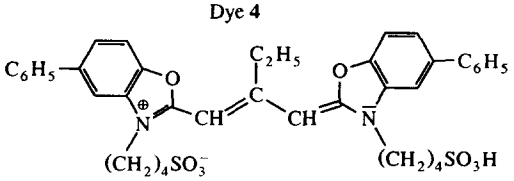

Dye 5

The dyes cover a pK_a range of 9.5 units. Dyes **1** and **2** were synthesized in our laboratory and dyes **3–5** were a gift from AGFA GEVAERT (Leverkusen). All dyes were used without further purification. Absorption and emission spectra were measured with a Specord M-400 spectrophotometer and a Perkin Elmer LS-50 fluorescence spectrometer, respectively. Fluorescence lifetimes were determined with an argon ion laser pumped and frequency doubled titanium–sapphire laser with excitation at 422 nm

(the high-energy side of the S_0–S_1 transition of the dyes). The overall response of the system was 50 ps.

3. Results

3.1. Monomeric dyes in sol–gel matrices

An overview of the spectroscopic data using the typical preparation procedure is given in Table 1. Since the results for both, formamide and dimethylsulfoxide, are similar, only the data for one DCCA are discussed. For **1** only the use of strong acids (HNO_3) as catalyst for the sol–gel preparation causes a disappearance of the long-wavelength absorption at 522.6 nm. The sample becomes yellow and in the UV-vis spectrum a new band appears at 320 nm (Fig. 1). The reaction is reversible because storage of the sample in ammonia atmosphere produces recoloration. In contrast, using KOH as catalyst, an absorption maximum at 526.6 nm is obtained (Fig. 1). Accordingly, a solution of **1** is also reversibly bleached in solution at low pH value by concomitant formation of an absorption band at 320 nm.

Also for **2** the disappearance of the long-wavelength absorption band is observed when HCl as catalyst was used for glass preparation. The decoloration is reversible storing the sample in ammonia atmosphere during gelation (Fig. 2) but, in contrast to **1**, with increasing gelation time this process becomes irreversible leading to a colorless sample without any absorption in the range 350–700 nm.

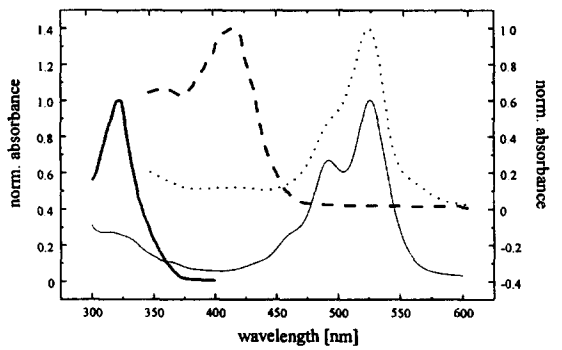

Fig. 1. Lower spectra: absorbance of dye **1** in sol–gel matrices: HNO_3 (bold solid line) catalysed KOH (thin solid line) catalysed. Upper spectra: absorbance of dye **2** in sol–gel matrices: HNO_3 (dashed line) catalysed, KOH/DMSO (dotted line) catalysed.

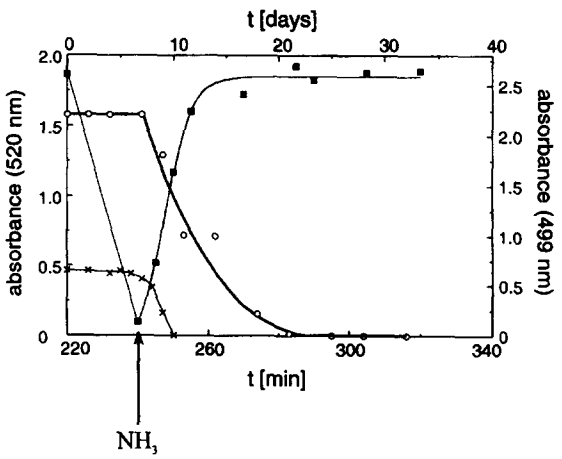

Fig. 2. Time dependence of the absorbance of dye **2**: (■) acid-catalysed (min), (×) base-catalysed (days); dye **4**: (○) base-catalysed.

Table 1
Photophysical properties of the cyanine dye monomer molecules

Dye	τ_0 (ns) (ϵ (L mol^{-1} cm^{-1}))	Sample [a]	λ_{max}^{abs} (nm)	λ_{max}^{em} (nm)	τ_f (ps)	ϕ_f
1	3.7 (112000)	E	522.6	635.0	< 10	< 0.01
		DCCA	526.6	595.2	19 (64), 315 (22), 2100 (14)	0.1
2	3.4 (123000)	E	520.1	538.8	123	0.04
		DCCA	522.7	584.1	198 (58), 1100 (42)	0.14
3	6.0 (110000)	E	553.3	581.8	38	0.01
		–	555.4	583.2	75 (37), 577 (37), 2600 (26)	0.15
		DCCA	557.5	593.7	30 (63), 343 (29), 1900 (8)	0.05
4	4.1 (130000)	E	498.8	515.5	64	0.02
		DCCA	499.3	522.2	78 (65), 260 (62), 1300 (3)	0.06
5 [b]	4.1 (122000)	E	504.9	523.2	76	0.02
		DCCA	507.0	528.7	94 (57), 436 (34), 1400 (9)	0.08

[a] E: ethanolic solution, –: sol-gel matrix without DCCA, DCCA: DCCA used for sol–gel preparation.
[b] A strong aggregation is observed in the sol-matrix prepared without DCCAs.

Looking at the UV-vis spectrum of **2** in aqueous solution at low pH values, the colorless species in the sol–gel matrix can be identified as the dicationic form. When basic catalysts or a pH buffer are used the absorbance at 523 nm remains unchanged but after a few days the protonated species is formed (Fig. 2).

In contrast to HCl, samples prepared with HNO_3 as catalyst exhibit a new band at 410 nm whereas the long-wavelength transition at 523 nm loses intensity (Fig. 1). Similar to **1**, this process can be reversed by storing the sample in ammonia atmosphere. However, the color irreversibly disappears again after a few days as already observed when KOH as catalyst is used (Fig. 2). Different preparation conditions were tested in order to prevent the protonation of the dye in sol–gel matrices which could be reached only if, according to the sample preparation described in the experimental part, DMSO as DCCA is added (Fig. 1).

Incorporating **3** and **5**, both possessing a pK_a value much lower than dye **2**, in the sol–gel matrix even without DCCA no formation of the dication is observed (Fig. 3). In contrast, a sample with **4** decolorizes after a few days (Fig. 2) but similar to dye **2** the addition of DMSO stabilizes the monocationic form in the sol–gel bulks.

In Table 1, the fluorescence lifetimes in ethanolic solution are compared with the lifetimes in the sol–gel matrices. In ethanolic solution, the dyes possess a lifetime in the range from < 10 up to 123 ps. A small second component with lifetime of about 200–600 ps was necessary to obtain good fits. In the sol–gel matrix the decay is multiexponential and

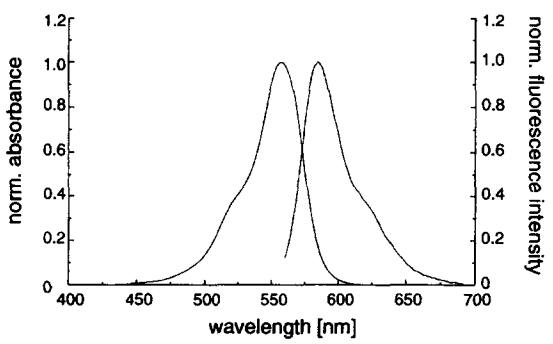

Fig. 3. Absorption and emission spectra of dye **3** embedded in the sol–gel matrix using KOH as catalyst.

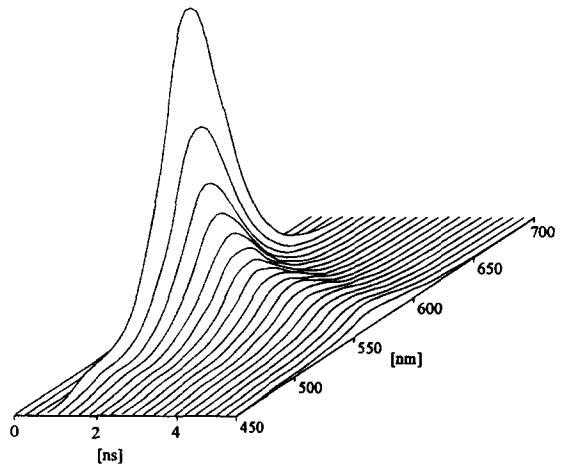

Fig. 4. Time-resolved emission spectra of **1** in the sol–gel matrix.

phenomenologically fitted by three exponentials. For samples without DCCA's the amplitude ratio of the shortest component a_1 and the longest component a_3 is about $a_1 : a_3 = 2$ whereas this ratio increases strongly up to 60 for samples prepared with formamide or DMSO. In the latter case, the short component has a decay time comparable to that in ethanolic solution. Also listed in Table 1 are the radiative lifetimes which are calculated from the absorption coefficient using the Strickler–Berg relation [20]. From the integrated decay curve an emission quantum yield is determined. In general, there is an increase in quantum yield of the dye in the sol–gel matrix compared to ethanolic solution, the stronger increase is observed for **3** without the addition of DCCA. Here the factor of increase is 15 as compared with the addition of DCCA which is 5.

Different geometrical restrictions of the molecules incorporated in the sol–gel matrix caused by different pores sizes are already indicated by the multiexponentiality. This may also cause a spectral shift of the emission spectrum which can be detected by time-resolved emission spectra. Since the emission maximum of **1** strongly depends on the geometrical structure in the first excited singlet state time-resolved emission spectra were recorded for this dye (Fig. 4). The emission spectra exhibit an increasing hypsochromic shift with increasing time. The total shift amounts to 5 nm between 200 ps and 2.5 ns. After 2.5 ns no further change in the spectral position is observed.

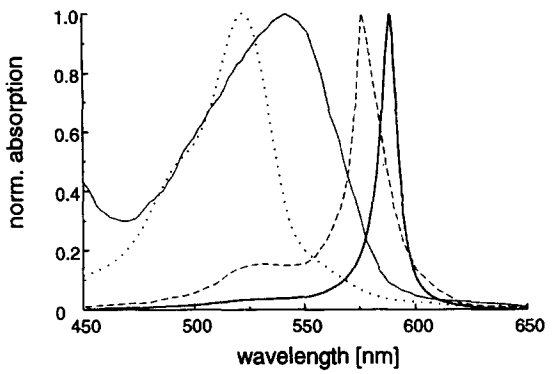

Fig. 5. Absorption spectrum of dye 2 in sol–gel matrices using KOH/DMSO stored at room temperature (dotted line) and at 60°C (thin solid line). Deposition of the sample in ammonia atmosphere leads to strong aggregation (dashed line) (for comparison also an absorption spectrum in aqueous solution is shown (bold solid line)).

3.2. J-aggregation in the sol–gel matrix

The aggregation behavior of the cyanine dyes was studied on **2**, a dye which is known to easily form J-aggregates without the intermediate formation of H-aggregates [21]. In a sample stored about 3 months at 60°C, aggregation takes place which, however, is completely different from the aggregation observed in solution (Fig. 5). The final peak centers at about 550 nm and the bandwidth of the aggregate absorption band is much higher than those observed in aqueous solution (230 cm^{-1}).

Table 2 shows the parallel course of the spectral shift and the decoloration process indicating that both the decoloration and the aggregate formation is due to the decrease in pore size during the stage of ageing. The aim to induce aggregation similar to that observed in solution is reached when storing a sol–gel sample in an ammonia atmosphere. The solution prepared according to the above mentioned procedure with the addition of DMSO exhibits a strong aggregation when deposited in an ammonia atmosphere right after preparation (Fig. 5). Both the absorption maximum (centered at 579 nm) and the bandwidth (410 cm^{-1}) are similar to J-aggregates in solution.

Table 2
Time dependence of absorbance and spectral position of the longest wavelength absorbance of dye 2 (the sample was prepared with KOH as catalyst and stored at 60°C)

t (days)	Absorbance	λ_{max} (nm)
6	2.25	518.7
21	0.075	521.4
26	0.033	545.2
29	0.031	550.0
32	0.028	544.4
34	0.026	546.8
40	0.027	545.0

4. Discussion

4.1. Protonation equilibria of monomeric dyes

Since all the samples were stored in the dark, light induced reactions such as photooxidation will be neglected in our considerations. In media of high acidity or basicity the long wavelength absorptivity of cyanine dyes is influenced by reactions with protons and BH nucleophiles [22,23]:

$$Dye^+ + BH \rightleftarrows DyeB + H^+, \quad (1)$$

$$Dye^+ + H^+ \rightleftarrows DyeH^{2+}. \quad (2)$$

Both reactions will lead to a disappearance of the longest wavelength transition due to interruption of the conjugated system. This allows one to follow the protonation easily by UV-vis spectroscopy.

Interactions of molecules with a sol–gel matrix can already occur when the reaction mixture is produced. In the second stage, if acid catalysts were used, the pH value strongly increases due to the evaporation of ethanol and the molecule embedded in the sol–gel matrix can react with "free" protons. Finally, in the stage of ageing interaction of the sol–gel walls with the incorporated molecules will start. Now, a protonation within the pores is possible because of the Lewis acidity of the Si–OH groups. Due to d-orbitals of the silicon atom the electrons of the oxygen are more strongly bonded on the silicon leading to high acidity of the proton [12]:

$$Si\text{–}OH \rightarrow Si\text{–}O\text{–}H \rightarrow Si\text{–}\overset{\delta^-}{O} \cdots \overset{\delta^+}{H}. \quad (3)$$

Table 3
pK_a values of the dyes used

Dye	pK_a value
1	4 [22]
2	7.66 [33]
3	−0.73 [34]
4	−1.83 [34]
5	−0.75 [34]

Depending on the TMOS/water ratio protonation can also occur through water molecules adsorbed on the surface:

$$\mathrm{Si{-}OH} + \mathrm{H_2O} \rightarrow \mathrm{Si{-}OH{-}OH_2}$$

$$\rightarrow \mathrm{Si{-}OH{-}\overset{\delta^-}{O}H \cdots \overset{\delta^+}{H}}\,. \qquad (4)$$

Since such protons are not "free", for protonation the approach of the molecules to the reactive centers is necessary. The tendency of protonation is given by the pK values of the cyanine dyes which are listed in Table 3. They increase in the direction oxazole < thiazole < quinoline < imidazole. Comparing the spectra of **1** in aqueous solution and in a sol–gel matrix the dication with an absorption band at 320 nm [23] is formed exclusively in HNO_3-catalysed samples. In contrast, dye **2** is protonated even when basic catalysts are used and results in a disappearance of the long-wavelength absorption (in aqueous solution with low pH value, only the absorption at 310 nm is visible). However, for samples of dye **2** catalysed with HNO_3 a new absorption band is observed at 410 nm. The two different absorption bands at 410 and 310 nm may be caused by protonation at different positions. In every case **2** is still colored in the starting solution but with increasing gelation time the color disappears independent of the catalyst used for the sol–gel preparation. Pre-agglomerates are, therefore, not responsible for the decoloration. Whereas the protonation is reversible in the beginning of gelation using HNO_3 as catalyst, probably due to an increasing pH value when ethanol evaporates, the time-dependent behavior of the absorptivity shows that irreversible decoloration processes take place much later (Fig. 2) indicating that the protonation is due to interactions between the dye and the silanol surface. This may also explain the irreversibility of the process since once incorporated in the pores the distance between the dye molecule and the silanol surface is fixed. Using basic catalysts protonation in the free solution is prevented but interaction of the dye with the sol–gel walls still occurs leading to the formation of the dicationic form. Further evidence for this hypothesis can be derived from the gas-phase acidity of the sol–gel surface which is defined as the Gibbs free energy of protonation dominated by the energy of deprotonation. Using the calculated values from Ref. [24], according to $pK_a = \Delta G/(2.3\ RT)$ with $\Delta G = 1576$ kJ/mol a pK_a value of 0.28 at $T = 20°C$ is obtained (this is not a property of the cavities but only the acidity of the silanol group). Such an acid matrix would lead to the formation of the dicationic form for the highly basic dye **2** but for dyes **3** and **5** the protonation would be prevented because of the lower basicity of the dyes. This is in agreement with the results since the long-wavelength absorption of **3** and **5** shows no decrease in the sol–gel matrix during ageing as compared to the starting solution.

However, the lack of protonation looking at **1** cannot be explained using the pK_a value. Despite its high pK_a value **1** is more stable than expected by the calculated acidity of the silanol groups. To understand this behavior not only the basicity but also the geometrical structure of the dye must be considered. As proven by X-ray analysis the two quinoline ring systems of **1** are twisted about 50° [25]. As the protonation takes place at the methine group in the cyanine chain of the dye we assume that the interaction of the silanol groups with dye molecules is prevented due to steric hindrance leading to a higher stability of the cationic form. It should be stressed that reaction with free protons is possible and only protonation according to Eq. (3) and Eq. (4) is suppressed. It is evident that this kind of stabilization is not possible for **2** which is almost planar as had been shown by X-ray analysis for the same chromophoric system having N,N-ethyl groups instead of N,N-sulfobutyl groups [26]. Due to its planarity this dye lies flat on the surface allowing optimal interaction with the silanol groups. The result may be of great importance for incorporating highly basic dyes in the sol–gel matrix by substituting dyes with bulky groups which hinders the approach on the silica surface. Thus the protonation of **1** using HNO_3 as catalyst is caused by decreasing the pH value when

ethanol evaporates. Accordingly, this process is reversible storing the sample in ammonia atmosphere.

Despite the low pK_a value for **4** the color disappears nearly after the same storage time as for **2** (Fig. 2). We believe that due to the high acidity of **4** the nucleophilic attack of a Si–O–Si unit is possible, in analogy to Eq. (1).

Stabilization of the cyanine dyes in the cationic form succeeds in all cases using drying control chemical agents which furthermore enhance glass quality. The influence of DCCAs on pore size can be estimated qualitatively from the fluorescence lifetimes listed in Table 1. In ethanolic solution all cyanine dyes show an emission lifetime between < 10 and 123 ps. Deviations from monoexponential behavior by cyanine dyes are discussed as a fast isomerization around the polymethine chain from the first excited singlet state. The deactivation channel of the excited molecule is, therefore, sensitive to viscosity and also to geometrical restrictions. The lifetimes should increase as the isomerization or torsion around the polymethine chain is hindered. The extraordinary short lifetime of **1** in ethanolic solution is in agreement with the measurements of Sibett et al. [19] and Tradwell et al. [27] and is explained by deviations from planarity of the two quinoline cycles.

In sol–gel matrices the multiexponentiality of the measured decay curves demonstrate that there is an inhomogeneous distribution of the trapping cages. While the short component corresponds to molecules with similar rotational freedom as in solution, the appearance of a long component in the sol–gel matrix is attributed to molecules which are fixed in the cages and whose radiationless deactivation of the first excited singlet state through rotation around the polymethine chain is prevented. This component should therefore approach the radiative lifetime which, indeed, is the case as compared with the radiative lifetimes calculated with the Strickler–Berg relation.

The fluorescence lifetimes reflect the differences in the sol–gel matrix prepared with and without DCCA. The differences are obvious from the ratios of the amplitudes $a_1 : a_3$ (a_1 amplitude of the shortest component, a_3 amplitude of the longest component). For samples prepared without additives the ratio $a_1 : a_3$ is about 2 for all the dyes showing the good reproducibility of the process. The ratio increases up to 60 for samples prepared with DMSO and the short fluorescence lifetime is comparable to that in solution. Using DCCAs, the pore size distribution shifts from smaller pores to pores which are large enough to enable molecular motion. Due to the higher porosity caused by additives the dye–silanol interaction is prevented and even the highly basic dye **2** does not react to the dicationic form. Accordingly, comparing the fluorescence quantum yields, which represent an indicator of the average pore size, in solution and in the sol–gel matrix for every dye an increase of a factor of 3 is obtained when additives are used. This is much less than the increase of 8 for **3** without additives. The maxima in samples prepared with DMSO are red-shifted up to 3 nm compared with ethanolic solution showing that the dye is surrounded by nonpolar molecules instead of the polar silica walls. Therefore, both the larger pore size and the microenvironment of the dye molecules embedded in sol–gel matrices prepared with DCCAs may contribute to the stabilization of the cationic form preventing the interaction with the sol–gel walls.

An exceptionally strong increase in the fluorescence quantum yield and lifetime in the sol–gel matrix prepared with DCCA is obtained for dye **1**. In ethanolic solution the low emission quantum yield and the short emission lifetime is probably due to enhanced internal conversion favoured by the twisting of the chromophores [28]. The increase in the sol–gel matrix may indicate, therefore, a more similar structure in the first excited singlet state as compared to the ground state caused by the geometrical size of the pores or the adsorption on the silica surface. This is supported by the fact that only for pseudoisocyanine the Stokes shift considerably decreases from 3390 cm^{-1} in ethanol to 2190 cm^{-1} in the sol–gel matrix.

If an increased planarity for **1** is responsible for the decreasing Stokes shift, their shift should also differ for molecules having different emission lifetimes. A short lifetime and a large Stokes shift correspond to large pores with a molecular geometry comparable to that in solution. With decreasing pore diameter the lifetime increases due to a stronger rigidization and, as indicated by steady-state spectroscopy, the Stokes shift decreases as a consequence of a less twisted geometry in the first excited singlet

state. An increase of the emission lifetime should, therefore, be connected with a decreasing Stokes shift which is indeed observed in time-resolved emission spectra. The emission maximum shifts about 5 nm from 575 to 570 nm with increasing decay time. Above 2.5 ns, a value which almost approaches the radiative lifetime, no further shift is observed. The molecules attributed to this lifetime fraction are already fixed in the pores and a further decrease in pore size has no effect on the photophysical properties of **1**.

4.2. Aggregation behavior

Generally, aggregation is supported by a high polarity of the environment. A sample of **2** prepared with DMSO and stored at 60°C shows a residual absorption intensity which remains almost unchanged after aggregation takes place (Table 2). This confirms the observation from Herz that pK_a are lowered by aggregation phenomena. Comparing the aggregate absorption band in solution and in a sol–gel matrix the absorption band in the sol–gel matrix is only slightly red-shifted as compared with the monomer absorption. Furthermore, the J-band is broad which indicates that the molecules cannot orientate themselves in an optimal way. The aggregate structure is disturbed. Although the largest pores of the sol–gel matrix were recently determined to be 15–25 nm and for acid catalysed samples 10–15 nm in diameter using atomic force microscopy [29], the spectral shift indicates that only two molecules interact with each other. The red-shift $\Delta\tilde{\nu}$ of the aggregate transition $\tilde{\nu}_A$ compared to the monomer transition $\tilde{\nu}_M$ can be approximately described by

$$\Delta\tilde{\nu} = \tilde{\nu}_A - \tilde{\nu}_M = \frac{1}{4\pi\epsilon_0}\frac{(N-1)}{N}\frac{2}{h}\frac{\langle M^2\rangle}{r^3}(1-3\cos^2\alpha), \quad (5)$$

where ϵ_0 is the permittivity in vacuum, h is Planck's constant and α is the angle between monomer transition dipole moment and aggregate axis. The distance between neighboring molecules r is 3.7 Å [30] and $\langle M^2\rangle$, the mean square of the monomer transition dipole moment (proportional to the integrated absorptivity of the monomer), is obtained from the absorption spectrum. The number of coupled molecules N in the aggregates was recently determined to an average value of 6.8 at room temperature [31]. The angle α can be calculated to 24°. Using this angle and the shift observed in the sol–gel matrix (1050 cm^{-1}) a value of about 2 is obtained for N.

The aggregation behavior strongly changes by changing the polarity of the environment or pore size. Comparing the aggregation of **2** embedded in a sol–gel matrix stored in air and in ammonia atmosphere we see that the ammonia causes a red-shift of the J-band nearly approaching that of an aqueous solution. However, one must take into account that ammonia also increases the pore size [32], thus not only the high polarity of ammonia is responsible for the aggregation.

5. Conclusion

The pK_a values of cyanine dyes give an indication of the stability of the monocationic form in porous glasses. Acid–base interactions between the silanol surface and cyanine dyes cause an attack at the cyanine chain leading to the formation of the colorless dicationic species. Therefore, only dyes with pK_a-values of about -0.5 are stable without further optimizing glass formation techniques. Using DCCAs for the sol–gel preparation, also the cationic form can be stabilized in the sol–gel matrix. Steric hindrance may suppress the dye–silanol interaction opening a new way of stabilizing even highly basic dyes in the sol–gel pores. Concerning the J-aggregation properties, we show the dependence of the J-aggregate formation on pore size and environment polarity.

Acknowledgement

This work was supported by the Deutsche Forschungsgemeinschaft (SFB 337) and Fonds der chemischen Industrie. One of us (UDR) wishes to thank Professor Reisfeld for providing the opportunity to work for three months at the Hebrew University of Jerusalem, Department of Inorganic and Analytical Chemistry.

References

[1] L.L. Hench and J.K. West, Chem. Rev. 90 (1990) 33.
[2] D. Avnir, V.R. Kaufman and R. Reisfeld, J. Non-Cryst. Solids 74 (1985) 395.
[3] A. Slama-Schwok, D. Avnir and M. Ottolenghi, J. Am. Chem. Soc. 113 (1991) 3984.
[4] M. Ueda, H.-B. Kim, T. Ikeda and K. Ichimura, J. Non-Cryst. Solids 163 (1993) 125.
[5] D. Avnir, D. Levy and R. Reisfeld, J. Phys. Chem. 88 (1984) 5956.
[6] R. Reisfeld, V. Chernyak and C.K. Jørgensen, Chimia 46 (1992) 148.
[7] R. Gvishi and R. Reisfeld, J. Non-Cryst. Solids 128 (1991) 69.
[8] V. Chernyak and R. Reisfeld, Sensors Mater. 4 (1993) 195.
[9] R. Reisfeld, R. Zusman, Y. Cohen and M. Eyal, Chem. Phys. Letters 147 (1988) 142.
[10] V. Chernyak, R. Reisfeld, R. Gvishi and D. Venezky, Sensors Mater. 2 (1990) 117.
[11] A.A. Ischenko, Russian Chem. Rev. 60 (1991) 865.
[12] B. Lebeau, N. Herlet, J. Livage and C. Sanchez, Chem. Phys. Letters 206 (1993) 15.
[13] S. De Boer, K.J. Vink and D.A. Wiersma, Chem. Phys. Letters 137 (1987) 99.
[14] M. Kasha, Radiation Res. 20 (1963) 55.
[15] F.C. Spano and S. Mukamel, Phys. Rev. A 40 (1989) 5783.
[16] H. Hada, R. Hanawa, A. Haraguchi and Y. Yonezawa, J. Phys. Chem. 89 (1985) 560.
[17] K. Misawa, H. Ono, K. Minoshima and T. Kobayashi, Appl. Phys. Letters 63 (1993) 577.
[18] T. Adachi and S. Sakka, J. Non-Cryst. Solids 99 (1988) 118.
[19] W. Sibbett, J.R. Taylor and D. Welford, J. Quantum Electron. QE-17 (1981) 500.
[20] S.J. Strickler and R.A. Berg, J. Chem. Phys. 37 (1962) 814.
[21] S. Mako, N. Kanamamaru and J. Tanaka, Bull. Chem. Soc. Japan 53 (1980) 3120.
[22] G. Buttgereit and G. Scheibe, Ber. Bunsenges. 69 (1965) 301.
[23] A.H. Herz, Phot. Sci. Eng. 18 (1974) 207.
[24] J. Sauer and J.R. Hill, Chem. Phys. Letters 218 (1994) 333.
[25] B. Dammeier and W. Hoppe, Acta Cryst. B 27 (1971) 2364.
[26] D.L. Smith and H.R. Luss, Acta Cryst. B 28 (1972) 2793.
[27] C.J. Tredwell and C.M. Keary, Chem. Phys. 43 (1979) 307.
[28] K. Teuchner, S. Daehne, J. Dresner and J. Prochorow, J. Luminescence 23 (1981) 413.
[29] M. Zevin, O. Wolfbeis and R. Reisfeld, unpublished results.
[30] U. De Rossi and S. Kirstein, unpublished results.
[31] U. De Rossi, S. Daehne and M. Lindrum, Langmuir, in press.
[32] R. Reisfeld, Advan. Nonradiat. Processes Solids (1991) 397.
[33] P. Beretta and A. Jabdi, Phot. Sci. Eng. 18 (1974) 197.
[34] U. Mazzucato, G. Cauzzo and G. Favaro, Ric. Sci. Rend. 33 (1963) 309.